

# Algorithm for molecular dynamics simulations of spin liquids

I. P. Omelyan,<sup>1</sup> I. M. Mryglod,<sup>1,2</sup> and R. Folk<sup>2</sup>

<sup>1</sup>*Institute for Condensed Matter Physics, 1 Svientsitskii Street, UA-79011 Lviv, Ukraine*

<sup>2</sup>*Institute for Theoretical Physics, Linz University, A-4040 Linz, Austria*

(November 18, 2018)

A new symplectic time-reversible algorithm for numerical integration of the equations of motion in magnetic liquids is proposed. It is tested and applied to molecular dynamics simulations of a Heisenberg spin fluid. We show that the algorithm exactly conserves spin lengths and can be used with much larger time steps than those inherent in standard predictor-corrector schemes. The results obtained for time correlation functions demonstrate the evident dynamic interplay between the liquid and magnetic subsystems.

Pacs numbers: 02.60.Cb; 75.40.Gb; 75.50.Mm; 76.50.+g; 95.75.Pq

Computer experiments remain an important tool for the prediction and theoretical understanding of various phenomena in magnetic materials. The methods of Monte-Carlo (MC) and molecular dynamics (MD) were intensively exploited over the years for the investigation of phase diagrams, critical phenomena, scaling, and the dynamic behavior of *lattice* systems such as the Ising, the XY, and the Heisenberg model [1–3].

The necessity to extend these studies to *disordered* models of magnetic liquids was motivated by a great amount of additional physical properties arising when both spin (orientational) and liquid (translational) degrees of freedom are taken into account [4–9]. The computer experiments for such systems have been restricted to MC simulations [5,7] in which only static quantities could be calculated. *Dynamic* phenomena, in particular, spin and density relaxations, and the effects connected with the mutual influence of magnetic and liquid subsystems can be investigated in MD simulations. Our special interest to this problem was also stimulated by the results obtained recently for a Heisenberg fluid within the hydrodynamic theory [9]. One of them was the prediction that the shape of magnetic dynamic structure factor can change *qualitatively* in comparison with the lattice model due to the *coupling* between the subsystems.

Until now, there have been *no* attempts to simulate spin liquids within the MD approach. This can be explained by the absence of an efficient MD algorithm for handling the corresponding equations of motion (EOM). The traditional numerical methods [10] for solving differential equations are unsuitable because they become highly unstable on time scales used in MD simulations. As has been well established for pure liquid systems [11,12], even standard predictor-corrector schemes are not efficient because of poor total energy conservation.

The properties of an acceptable algorithm for long-time observations over a many-body system should be: stability, accuracy, speed and ease of implementation. There exists only a small group of integrators satisfying these criteria. An important one is the velocity Verlet (VV) algorithm [13,14] which allows a high accuracy with

minimal costs in terms of time-consuming force evaluations. However, the VV and other similar schemes [11,15] were designed to simulate pure liquid dynamics. In the case of magnetic liquids the situation is more complicated since the translational positions and momenta are *coupled* with spin orientations in a characteristic way and, hence, all these dynamical variables must be considered simultaneously. This requires substantial revision of the liquid dynamic algorithms.

Recently, new algorithms have been devised for spin dynamics simulations of lattice systems [16]. They are based (like the VV integrator) on the Suzuki-Trotter (ST) decomposition method and appear to be much more efficient than predictor-corrector schemes. These algorithms are applicable to spin systems if the decomposition on two (or several) noninteracting sublattices is possible. However, they cannot be used for models with arbitrary spatial spin distributions and, therefore, not for spin liquids.

In this Letter we develop the idea of using ST-like decompositions for spin liquid dynamics and derive the desired MD algorithm. This allows quantitative measurement of dynamical structure factors of a Heisenberg fluid. The main result obtained (reflecting the influence of the liquid subsystem on spin dynamics) is the identification of a new propagative sound-like mode in the spectrum of collective longitudinal spin excitations.

Consider a classical system composed of  $N$  magnetic particles of mass  $m$ , described by the Hamiltonian [7,8]

$$H = \sum_{i=1}^N \frac{m\mathbf{v}_i^2}{2} + \sum_{i<j}^N \left[ \Phi(r_{ij}) - J(r_{ij}) \mathbf{s}_i \cdot \mathbf{s}_j \right]. \quad (1)$$

Here  $\mathbf{r}_i$  and  $\mathbf{v}_i$  are the translational position and velocity, respectively, of particle  $i$  carrying spin  $\mathbf{s}_i$ . The liquid potential is denoted by  $\Phi(r_{ij})$ , and  $J(r_{ij}) > 0$  is the exchange integral for a pair of spins with interparticle distance  $r_{ij}$ . The classical approach treats  $\mathbf{s}_i$  as a three-component continuous vector with a fixed length for each site  $i$ . We put for convenience  $|\mathbf{s}_i| = 1$ , so that  $J$  is measured in energy units.

In order to study the *dynamic* properties, the equations of motion given by  $d\boldsymbol{\rho}/dt = L\boldsymbol{\rho}(t)$  must be integrated numerically, where

$$L = \sum_{i=1}^N \left( \mathbf{v}_i \cdot \frac{\partial}{\partial \mathbf{r}_i} + \mathbf{a}_i \cdot \frac{\partial}{\partial \mathbf{v}_i} + [\boldsymbol{\omega}_i \times \mathbf{s}_i] \cdot \frac{\partial}{\partial \mathbf{s}_i} \right) \equiv \sum_{i=1}^N (L_{\mathbf{r}_i} + L_{\mathbf{v}_i} + L_{\mathbf{s}_i}) \equiv L_{\mathbf{r}} + L_{\mathbf{v}} + L_{\mathbf{s}}, \quad (2)$$

is the Liouville operator, i.e.,  $L\boldsymbol{\rho} = [\boldsymbol{\rho}, H]$  with  $[\ , \ ]$  being the Poisson bracket;  $\boldsymbol{\rho} \equiv \{\mathbf{r}_i, \mathbf{v}_i, \mathbf{s}_i\}$  denotes the full set of microscopic phase variables;  $\mathbf{a}_i = \mathbf{f}_i/m$  and  $\boldsymbol{\omega}_i = -\mathbf{g}_i/\hbar$  are the acceleration and local Larmor frequency, respectively, with  $\mathbf{f}_i = -\sum_{j(j \neq i)} [d\Phi(r_{ij})/dr_{ij} - dJ(r_{ij})/dr_{ij} \mathbf{s}_i \cdot \mathbf{s}_j] \mathbf{r}_{ij}/r_{ij}$  and  $\mathbf{g}_i = \sum_{j(j \neq i)} J(r_{ij}) \mathbf{s}_j$  being the force and internal magnetic field. Note that the operators  $L_{\mathbf{r}}$ ,  $L_{\mathbf{v}}$  and  $L_{\mathbf{s}}$  act only on position, velocity and spin, respectively, and the quantum Poisson bracket was used [8,16] to obtain  $L_{\mathbf{s}}$ .

The solutions can be cast in the form  $\boldsymbol{\rho}(t+h) = e^{Lh} \boldsymbol{\rho}(t) = e^{(L_{\mathbf{r}}+L_{\mathbf{v}}+L_{\mathbf{s}})h} \boldsymbol{\rho}(t)$ , where  $h$  is the time step. Since the exponential propagator  $e^{Lh}$  cannot be evaluated exactly, one introduces some approximations which take advantage of the smallness of  $h$ . Assuming for the moment that spin variables are frozen, i.e. setting  $L_{\mathbf{s}} \rightarrow 0$ , we come to the usual (liquid-like) EOM. They can be solved in a quite efficient way using the second-order VV integrator [13,14] which is based on the ST formula  $e^{(L_{\mathbf{r}}+L_{\mathbf{v}})h} = e^{L_{\mathbf{v}}h/2} e^{L_{\mathbf{r}}h} e^{L_{\mathbf{v}}h/2} + \mathcal{O}(h^3)$ . Taking into account the fact that this formula is valid for arbitrary two operators and unfreezing now the spin variables, we obtain immediately:  $e^{(L_{\mathbf{r}}+L_{\mathbf{v}}+L_{\mathbf{s}})h} = e^{L_{\mathbf{v}}h/2} e^{(L_{\mathbf{r}}+L_{\mathbf{s}})h} e^{L_{\mathbf{v}}h/2} + \mathcal{O}(h^3)$ , where the sum  $L_{\mathbf{r}} + L_{\mathbf{s}}$  was treated as one operator. The spin-position sub-propagator can further be decomposed in a similar way,  $e^{(L_{\mathbf{r}}+L_{\mathbf{s}})h} = e^{L_{\mathbf{r}}h/2} e^{L_{\mathbf{s}}h} e^{L_{\mathbf{r}}h/2} + \mathcal{O}(h^3)$ , resulting in a full propagation of the form

$$\boldsymbol{\rho}(t+h) = e^{L_{\mathbf{v}}h/2} e^{L_{\mathbf{r}}h/2} e^{L_{\mathbf{s}}h} e^{L_{\mathbf{r}}h/2} e^{L_{\mathbf{v}}h/2} \boldsymbol{\rho}(t) + \mathcal{O}(h^3). \quad (3)$$

Note that other decompositions are also possible, but then the local fields  $\mathbf{g}_i$  and/or forces  $\mathbf{f}_i$  have to be updated (the most time-consuming operations) more frequently, which reduces the efficiency of the computations.

The main idea of the decompositions is to obtain sub-propagators which can be evaluated *analytically*. It can be shown [14] that the position  $e^{L_{\mathbf{r}}\tau} = \prod_i e^{L_{\mathbf{r}_i}\tau}$  and velocity  $e^{L_{\mathbf{v}}\tau} = \prod_i e^{L_{\mathbf{v}_i}\tau}$  propagations represent shift operators, namely,  $e^{L_{\mathbf{r}_i}\tau} \mathbf{r}_i = \mathbf{r}_i + \mathbf{v}_i\tau$  and  $e^{L_{\mathbf{v}_i}\tau} \mathbf{v}_i = \mathbf{v}_i + \mathbf{a}_i\tau$ . Since the components  $L_{\mathbf{r}}$  and  $L_{\mathbf{v}}$  (as well as  $L_{\mathbf{s}}$ ) do not commute, such shifts must be performed in a rigorous order (as specified by Eq. (3)) and applied to the current values of  $\mathbf{r}_i$  and  $\mathbf{v}_i$  within the time step.

The spin subdynamics is described in Eq. (3) by the exponential operator  $e^{L_{\mathbf{s}}h}$ . This operator has no simple explicit form, because the Larmor frequency  $\boldsymbol{\omega}_i$  for

each particle depends in general on the orientations of all other spins of the system. The explicit solution, nevertheless, may be found as follows. Since all the partial components  $L_{\mathbf{s}_i}$  do not commute each other, it is quite natural to find an ST-like decomposition for the whole set of these operators. This results to the expression

$$e^{L_{\mathbf{s}}h} = e^{L_{\mathbf{s}_1}h/2} \dots e^{L_{\mathbf{s}_{N-1}}h/2} e^{L_{\mathbf{s}_N}h} e^{L_{\mathbf{s}_{N-1}}h/2} \dots e^{L_{\mathbf{s}_1}h/2}, \quad (4)$$

which constitutes an ST analog for arbitrary number of operators and is accurate to the same order  $\mathcal{O}(h^3)$  as the terms already truncated. Again, other  $\mathcal{O}(h^3)$  decompositions may be introduced. However, only Eq. (4) will lead to a scheme with *minimal* number of local field recalculations.

The problem is now considerably simplified because, according to Eq. (4), each current value of  $\mathbf{s}_i$  is updated spin by spin at a fixed instantaneous Larmor frequency  $\boldsymbol{\omega}_i$ , and this case allows analytical solutions:  $e^{L_{\mathbf{s}_i}\tau} \mathbf{s}_i(t) = \mathbf{D}_i(t, \tau) \mathbf{s}_i(t)$ . Here  $\mathbf{D}_i(t, \tau) = \mathbf{I} + \mathbf{W}_i \sin(\omega_i\tau) + \mathbf{W}_i^2 (1 - \cos(\omega_i\tau))$  denotes an orthonormal ( $\mathbf{D}\mathbf{D}^+ = \mathbf{I}$ ) matrix of rotation around axis  $\boldsymbol{\omega}_i$  on angle  $\omega_i\tau$  and  $\mathbf{W}_i = \mathbf{W}(\hat{\boldsymbol{\omega}}_i)$  is a skewsymmetric matrix ( $\mathbf{W}_{\alpha\beta} = -\mathbf{W}_{\beta\alpha}$ ) with  $\mathbf{W}_{XY} = -\hat{\omega}_Z$ ,  $\mathbf{W}_{XZ} = \hat{\omega}_Y$ ,  $\mathbf{W}_{YZ} = -\hat{\omega}_X$  and  $\hat{\boldsymbol{\omega}} = \boldsymbol{\omega}/\omega$ . Since the decompositions used are correct within an uncertainty of order  $\mathcal{O}(h^3)$ , the trigonometric functions can be replaced by their rational counterparts (see, e.g., [17]),  $\cos \xi = (1 - \xi^2/4)/(1 + \xi^2/4) + \mathcal{O}(\xi^3)$  and  $\sin \xi = \xi/(1 + \xi^2/4) + \mathcal{O}(\xi^3)$ , which maintain the orthonormality of  $\mathbf{D}$  and are more efficient for the computations. Then the spin rotation reduces to

$$e^{L_{\mathbf{s}_i}\tau} \mathbf{s}_i(t) = \left( \mathbf{s}_i(t) + [\boldsymbol{\omega}_i \times \mathbf{s}_i(t)]\tau + \frac{\tau^2}{2} (\boldsymbol{\omega}_i (\boldsymbol{\omega}_i \cdot \mathbf{s}_i(t)) - \frac{1}{2} (\boldsymbol{\omega}_i \cdot \boldsymbol{\omega}_i) \mathbf{s}_i(t)) \right) / \left( 1 + \left( \frac{\omega_i \tau}{2} \right)^2 \right). \quad (5)$$

This completes the new algorithm.

We note that our basic EOM are time-reversible and exact solutions behave symplectically. As can be shown, the algorithm derived reproduces these features, even though the trajectories are generated with a limited accuracy. Indeed, the initial propagator was decomposed (Eqs. (3) and (4)) into subparts symmetrically, and, as a consequence, the final expressions for  $\mathbf{r}_i$ ,  $\mathbf{v}_i$  and  $\mathbf{s}_i$  will be invariant with respect to the transformation  $h \rightarrow -h$ . Furthermore, simple shifts (applied separately in position and velocity space) do not change the phase volume. These properties are very important for our purpose because, as is now well established [11,14], the stability of an algorithm normally follows from its time reversibility and symplecticity. Another nice property of the algorithm is its exact conservation of spin lengths (rotations given by Eq. (5) do not change the norm of vectors) that is crucial for the class of models considered.

In our MD study of the Heisenberg fluid, we have used the Yukawa potential [7],  $J(r) = (\epsilon\sigma/r) \exp[(\sigma - r)/\sigma]$ , and a soft-core potential [11],  $\Phi(r) = 4\epsilon[(\sigma/r)^{12} - (\sigma/r)^6] + \epsilon$  at  $r < 2^{1/6}\sigma$  and  $\Phi(r) = 0$  otherwise,

for the description of spin and liquid interactions with the intensities  $\epsilon$  and  $\varepsilon$ , respectively. The function  $J(r)$  was truncated at  $R = 2.5\sigma$  and shifted to be zero at the truncation point to avoid force singularities. The simulations were carried out for  $N = 1000$  particles (employing periodic boundary conditions) at a reduced density  $n^* = N\sigma^3/V = 0.6$ , a reduced temperature  $T^* = k_B T/\epsilon = 1.5 < T_c^*$  (where  $T_c^* \simeq 2.06$  is the temperature of ferromagnetic transition [18]), a reduced core intensity  $\varepsilon/\epsilon = 1$ , and a *dynamical coupling parameter*  $d = \sigma(m\epsilon)^{1/2}/\hbar = 2$ . This last parameter presents, in fact, the ratio  $\tau_{tr}/\tau_s$ , where  $\tau_{tr} = \sigma(m/\epsilon)^{1/2}$  and  $\tau_s = \hbar/\epsilon$  are the characteristic time intervals of varying translational and spin variables, respectively. Since we are investigating a *ferrophase* and dealing with a *microcanonical* (NVES) ensemble, a non-zero magnetization of the system must be specified additionally. This quantity was taken from our single MC simulation [18],  $\langle \mathbf{S} \rangle_0/N = 0.6536 \pm 0.0001$ , where  $\langle \cdot \rangle_0$  denotes the canonical averaging. All test runs were started from an identical well equilibrated configuration. The recalculation of local magnetic fields (during spin subdynamics (4)) took approximately the same processor time as that of translational forces, spending in total 0.5 sec per step on the Origin 2000 workstation. It is worth emphasizing that contrary to spin lattice dynamics [16] (when auxiliary MC cycles are involved to generate equilibrium configurations as initial conditions for the EOM), the equilibration of our system can be performed within NVES MD simulations exclusively (at the specified value for  $\mathbf{S} \equiv \langle \mathbf{S} \rangle_0$ ). This is possible because of the *energy exchange* between the spin and liquid subsystems.

Symmetries of Hamiltonian (1) impose conservation laws on the total momentum  $\mathbf{P} = m \sum_i \mathbf{v}_i$ , total spin  $\mathbf{S} = \sum_i \mathbf{s}_i$  and total energy  $E \equiv H$ . These three integrals of motion cannot be conserved perfectly at the same time within any approximate scheme known. This is a typical situation in MD simulations. The MD results for the total energy  $E^* = E/\epsilon$  (subsets (a)-(d)) and total spin  $S$  (subsets (e)-(h)) as functions of the length of the simulations are presented in Fig. 1. Four time steps, namely,  $h^* = h/\tau_{tr} = 0.00125, 0.0025, 0.005$  and  $0.01$ , were used to integrate the EOM (solid curves). These results are compared with those obtained by us using the well established Adams-Bashforth-Moulton (ABM) predictor-corrector scheme [10] (dashed curves in subsets (a) and (b)). As can be seen from Fig. 1a, the ABM integrator fulfills energy conservation up to a similar accuracy as our algorithm at the smallest time step  $h^* = 0.00125$ . However, for larger step sizes (see Fig. 1b) the ABM scheme is unstable and, thus, cannot be used. Note that very small step sizes are impractical because then too much time-consuming force and field evaluations have to be done during the typical observation times.

No systematic drift in  $E(t)$  and  $S(t)$  was observed within our algorithm at time steps up to  $h^* = 0.01$  over a length of  $t/h = 100\,000$ . The precision of the algorithm was measured in terms of the ratio  $\Gamma_E =$

$(\langle (E(t) - E(0))^2 \rangle / \langle (U(t) - U(0))^2 \rangle)^{1/2}$  of total and potential ( $U$ ) energy fluctuations. Taking into account that for our system  $(\langle (U(t) - U(0))^2 \rangle)^{1/2} \approx 0.0335$ , we have obtained:  $\Gamma_E \approx 0.12\%, 0.28\%, 0.98\%$  and  $7.7\%$  for the time steps  $h^* = 0.00125, 0.0025, 0.005$  and  $0.01$ , respectively. In order to reproduce properly the features of microcanonical ensembles the ratio  $\Gamma_E$  should not exceed a few per cent. As we can see, time steps of  $h^* \leq 0.01$  satisfy this requirement and, thus, they can be used for precise calculations.

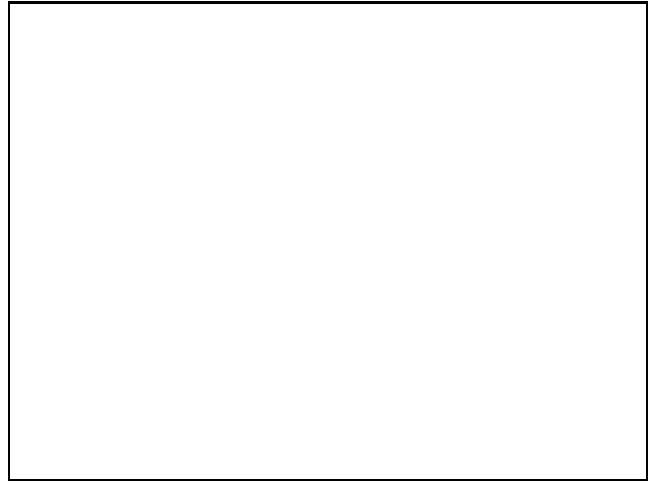


FIG. 1. Reduced total energy  $E^*(t)/N$  [(a)-(d)] and magnetization  $S(t)/N$  [(e)-(h)] per spin as functions of the observation time obtained within the decomposition [solid curves] and predictor-corrector [dashed curves in (a) and (b)] algorithms at four fixed time steps:  $h^* = 0.00125, 0.0025, 0.005$ , and  $0.01$ . The values  $E^*(0)/N$  and  $S(0)/N$  are plotted by the horizontal thin lines.

Note that the decomposition and ABM methods conserve the total momentum  $\mathbf{P}$  to within machine accuracy. The reason is that all velocities are updated simultaneously and the interparticle forces are evaluated exploiting Newton's third law. For similar reasons, the ABM integration maintains the total magnetization  $\mathbf{S}$  (but it does not conserve spin lengths). In our scheme the magnetization is not conserved exactly. However, the fluctuations appear to be very small (see Fig. 1e-1h) and lead to the values  $(\langle (\mathbf{S}(t) - \mathbf{S}(0))^2 \rangle)^{1/2} \simeq 10^{-7}, 5 \cdot 10^{-7}, 2 \cdot 10^{-6}$  and  $10^{-5}$  at  $h^* = 0.00125, 0.0025, 0.005$  and  $0.01$ , respectively.

The spectra  $F(k, \omega) = \frac{1}{2\pi} \int_{-\infty}^{\infty} F(k, t) e^{-i\omega t} dt$  of the spin-spin  $F_{ss}^{L,T}(k, t) = \langle \sum_{i,j} \mathbf{s}_i^{L,T}(0) \cdot \mathbf{s}_j^{L,T}(t) n_{ij}(\mathbf{k}, t) \rangle$ , density-density  $F_{nn}(k, t) = \langle \sum_{i,j} n_{ij}(\mathbf{k}, t) \rangle$  and spin-density  $F_{sn}^L(k, t) = \langle \sum_{i,j} \mathbf{s}_i^L(0) n_{ij}(\mathbf{k}, t) \rangle \equiv F_{ns}^L(k, t)$  time correlation functions are shown in Fig. 2. The superscripts (L) and (T) refer to the longitudinal and transverse components of  $\mathbf{s}_i$  with respect to the vector  $\mathbf{S}$ , and  $n_{ij}(\mathbf{k}, t) = N^{-1} \exp\{i\mathbf{k} \cdot (\mathbf{r}_i(0) - \mathbf{r}_j(t))\}$ . These functions were obtained within our decomposition integration at

$h^* = 0.005$ , and the microcanonical averaging  $\langle \rangle$  was taken over 100 000 steps for each of 10 independent runs. A dimensionless representation has been used for  $F^*(k, \omega) = F(k, \omega)/\tau_{\text{tr}}$  with  $\omega^* = \omega\tau_{\text{tr}}$ ,  $k^* = k/k_{\text{min}}$  and  $k_{\text{min}} = 2\pi/V^{1/3}$ .

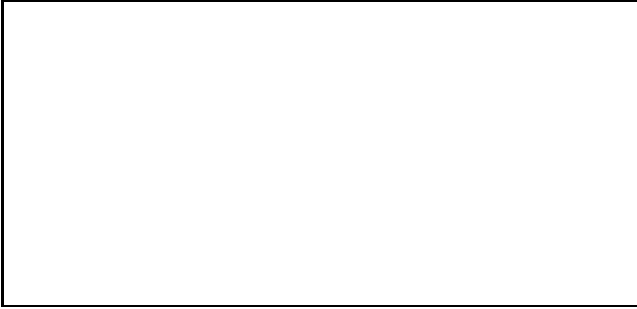


FIG. 2. Transverse (a) and longitudinal (b) spin-spin, density-density (c), and spin-density (d) functions for a Heisenberg fluid versus frequency  $\omega^*$ . The curves corresponding to the wavenumbers  $k^* = 1, 2, 3$ , and 5 are marked by "1", "2", "3", and "5", respectively.

One peak can be identified for the function  $F_{ss}^T(k, \omega)$  at each wavevector  $k$ . This peak is very sharp at small  $k$  and shifts to the right with increasing  $k$ . Such a quasiparticle behavior should be associated with the existence of *transverse spin waves* in the spin liquid. Up to three maxima were observed for the component  $F_{ss}^L(k, \omega)$ . While the first maximum at  $\omega = 0$  corresponds to pure diffusive processes, the position of the second one coincides with that of the transverse spin wave peak, indicating the possibility of propagating *longitudinal spin waves* as well which, however, are damped much stronger. The origin of the third maximum in  $F_{ss}^L(k, \omega)$  can be explained by the direct influence of the liquid subsystem on the spin one, because its position coincides with a peak position in  $F_{nn}(k, \omega)$ . This last peak should be associated with propagative *sound modes* well established for liquid systems [19], whereas a maximum of  $F_{nn}(k, \omega)$  at  $\omega = 0$  represents the well-known diffusive *heat mode*. The function  $F_{sn}^L(k, \omega)$  behaves similarly to  $F_{nn}(k, \omega)$ . In general the results obtained are in good agreement with the predictions of Ref. [9]. The additional possibility of longitudinal spin wave propagations in magnetic liquids at sound frequency can be considered as a new effect which has yet to be observed experimentally. Similar effect was found also [18] in our MD calculations performed for model (1) at a higher temperature  $T > T_c$  at the presence of an external magnetic field. Taking into account the theoretical results of Ref. [9] allows us to state that in the both cases considered the Brillouin sound peaks appear in  $F_{ss}^L(k, \omega)$  due to magnetostriction caused by spin ordering.

In conclusion, we list the chief advantages of the new algorithm over existing numerical schemes: (i) time-reversibility and symplecticity; (ii) explicitness (no iteration); (iii) exact conservation of spin lengths; (iv) much more accuracy in total energy conservation. Moreover, its excellent stability (allowing applications with much larger time steps) may lead to a substantial improvement of the speed of MD simulations for magnetic liquids. It can also be used for lattices (then only Eqs. (4) and (5) must be employed) with arbitrary structures. These and related problems will be considered in a separate publication.

Part of this work was supported by the Fonds zur Förderung der wissenschaftlichen Forschung under Project No. P12422-TPH.

- 
- [1] H.G. Evertz and D.P. Landau, Phys. Rev. B **54**, 12302 (1996).
  - [2] A. Bunker, K. Chen, and D.P. Landau, Phys. Rev. B **54**, 9259 (1996).
  - [3] D.P. Landau and M. Krech, J. Phys. Cond. Mat. **11**, R179 (1999).
  - [4] K. Handrich and S. Kobe, *Amorphe Ferro- und Ferrimagnetika* (Akademika-Verlag, Berlin, 1980).
  - [5] E. Lomba, J.J. Weis, N.G. Almarza, F. Bresme, and G. Stell, Phys. Rev. E **49**, 5169 (1994).
  - [6] J.M. Tavares, M.M.T. Gama, P.I.C. Teixeira, J.J. Weis, and M.J.P. Nijmeijer, Phys. Rev. E **52**, 1915 (1995).
  - [7] M.J.P. Nijmeijer, J.J. Weis, Phys. Rev. E **53**, 591 (1996).
  - [8] I.M. Mryglod and R. Folk, Physica A **234**, 129 (1996).
  - [9] I. Mryglod, R. Folk, S. Dubyk, and Yu. Rudavskii, Physica A **277**, 389 (2000).
  - [10] R.L. Burden and J.D. Faires, *Numerical Analysis*, 5th ed. (PWS Publishing, Boston, 1993).
  - [11] M.P. Allen and D.J. Tildesley, *Computer Simulation of Liquids* (Clarendon, Oxford, 1987).
  - [12] I.P. Omelyan, Phys. Rev. E **58**, 1169 (1998).
  - [13] W.C. Swope, H.C. Andersen, P.H. Berens, and K.R. Wilson, J. Chem. Phys. **76**, 637 (1982).
  - [14] D. Frenkel and B. Smit, *Understanding Molecular Simulation: from Algorithms to Applications* (Academic Press, New York, 1996).
  - [15] M. Tuckerman, B.J. Berne, and G.J. Martyna, J. Chem. Phys. **97**, 1990 (1992).
  - [16] M. Krech, A. Bunker, and D.P. Landau, Comput. Phys. Commun. **111**, 1 (1998).
  - [17] A. Dullweber, B. Leimkuhler, and R. McLachlan, J. Chem. Phys. **107**, 5840 (1997).
  - [18] R. Folk, I.M. Mryglod, and I.P. Omelyan [unpublished].
  - [19] I.M. Mryglod and I.P. Omelyan, Mol. Phys. **91**, 1005 (1997).

